Mean-Field Study of Kondo Phase Diagram

Part III Project Report

Supervisors: Claudio Castelnovo & Garry Goldstein

May 14, 2018

Abstract

Phase diagram predictions for the Kondo model from mean-field theory are known to disagree with the exact *Bethe ansatz* result by failing to describe the *crossover* into the Kondo phase. In this project we apply a new variation of mean-field theory to this problem, which differs in the novel way that it implements constraints into the Lagrangian through the introduction of an auxiliary system. This implementation introduces a new free parameter which has previously been shown to enable a better a prediction of the characteristic energy scale (the Kondo temperature) and other derived properties of the system at zero temperature. Here we show that this free parameter must necessarily be made temperature dependent if it is to reproduce basic features of the finite temperature behaviour, but that after making this allowance it is possible to increase the order of the otherwise second-order phase transition. Nevertheless, it is shown that this added freedom is still not enough to avoid a phase transition entirely, as is typical of other mean-field theories.

1 Introduction

Metallic systems with localised magnetic impurities have, over the years, been the subject of much research in condensed matter physics, falling under the broader branch of strongly correlated systems which are characterised by interactions being significant in comparison to the kinetic energy dispersion (bandwidth).

The enormous theoretical challenge of studying strongly correlated systems, with their broad ranges of energy scales, means that one often turns to effective models to describe the low energy behaviour, introducing strict constraints that arise after *projecting out* higher energy terms. One such effective model, studied in this project, is the Kondo model. This describes conduction electrons coupled to a (single) localised spin at the origin as a model for the dilute magnetic impurities that are sometimes present in a metal.

The many rich features of the general Kondo problem have been widely studied, with some simpler formulations being amenable to an exact solution via Bethe ansatz techniques. Often times, however, it is necessary to employ approximate methods to obtain results in more general cases, one such method being mean-field theory.

Use of mean-field theory is far from ideal, however, since current formulations applied to the Kondo impurity model are known to give results in disagreement with the Bethe ansatz solution for a characteristic energy of the problem known as the Kondo temperature T_K and (by extension) the magnetic susceptibility at zero temperature. The heat capacity is also greatly underestimated by existing mean-field methods. Recently, a new mean-field approach [2] has been proposed by Garry Goldstein, Claudio Castelnovo (supervising the project) and Claudio Chamon which has given improved estimates of these quantities, which may be a sign that this new variation is indeed an improvement over existing formulations. We are therefore interested in the Kondo problem to the extent that it provides a well-known platform for testing and assessing the potential efficacy of this new mean-field method.

One significant aspect of the Kondo model that existing mean-field formulations have thus far failed to capture properly is the crossover from a Kondo to a paramagnetic phase in the temperature-field phase diagram, instead predicting a phase transition as in Figure 1. The primary aim of this project is therefore to extend this new formulation to finite temperature, specifically to the temperature-field phase diagram and see whether a phase transition or a crossover is predicted. If the predicted behaviour is found to align with that of the exact Bethe ansatz solution, then the case for this new mean-field approach as an alternative to existing formulations would be greatly strengthened.

The report is structured as follows: Section 2 introduces the theoretical ideas underpinning the project; Section 3 contains the main finite temperature investigation; Section 4 gives a brief account of the behaviour at finite magnetic field and Section 5 concludes with an overview of the main results of the project.

2 Theoretical Background

This new approach builds on quite a few established techniques in strongly correlated systems which we shall include in this section for completeness.

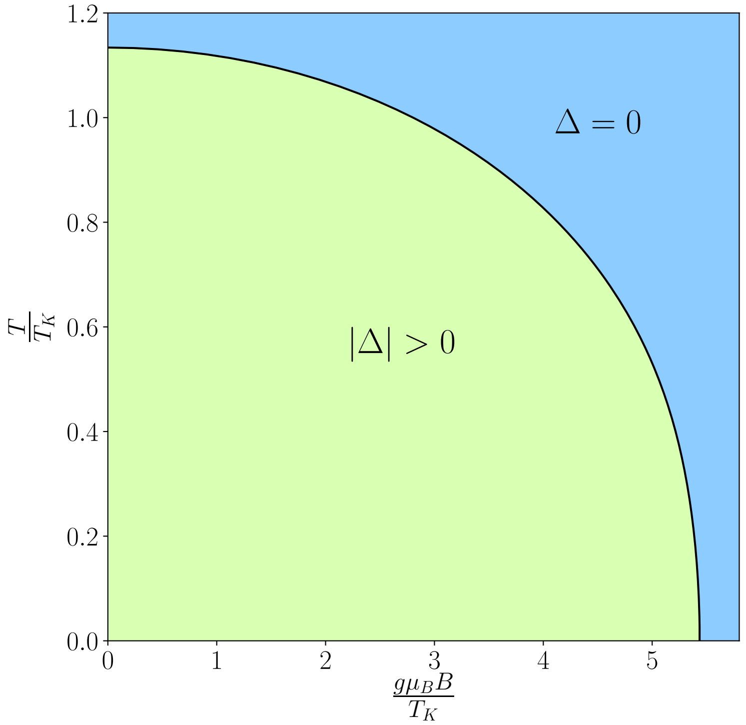

Figure 1: A representative phase diagram obtained from another (Read-Newns) mean-field approach (with calculations found in [1]), which shows a distinct phase transition between two phases. The Kondo temperature T_K is used to make quantities dimensionless.

2.1 Local Moments

The Kondo model made its first appearance in 1964 when theorists were attempting to explain puzzling experimental observations made 30 years earlier that certain metals containing magnetic impurities showed minima in their resistivity as a function of temperature. Remarkably, this effect is present even for very small concentrations of magnetic ions, in which unpaired electrons reside in highly localised orbitals (such as the d- or f-shells) [1].

In isolation, one would expect such local moments to show the usual signs of Curie paramagnetism (where $\chi \propto \frac{1}{T}$). What is found for these materials, however, is that as the temperature is lowered, the local moments begin to interact so strongly with conduction electrons in the metallic host that they become screened, removing their internal degrees of freedom to form a Fermi-liquid. In this strongly-coupled regime, the conduction and impurity electrons entangle to form a spin-singlet that behaves as a resonant scattering centre, providing an explanation for the observed functional form of the resistivity [3].

Here, the characteristic energy scale that sets this crossover is the *Kondo temperature* T_K (below which $\chi \propto \frac{1}{T_K}$). This dependence on energy scale meant that the Kondo effect played a large rôle in the development of the renormalisation group, which was later used to shed further light on this problem by relating it to the *Anderson model* for moment formation.

2.2 Kondo Model

In its simplest single impurity flavour, the Kondo model has the following Hamiltonian:

$$H_{\text{Kondo}} = \sum_{\boldsymbol{k},\sigma} \epsilon_{\boldsymbol{k}} c^\dagger_{\boldsymbol{k},\sigma} c_{\boldsymbol{k},\sigma} + J\vec{S}\cdot\vec{s}(0), \tag{1}$$

in which there is a kinetic energy contribution from the conduction electrons $c_{\boldsymbol{k},\sigma}$ (with $\sigma \in \{\uparrow,\downarrow\}$) as well as a term describing an antiferromagnetic coupling between a spin localised at the origin and the spin density of conduction electrons at that point.[1] (This model may be considered to be the limit of moments being sufficiently dilute such that they do not interact with each other, thus becoming a one-dimensional problem.)

2.3 The Path Integral

The theoretical calculations of this project are framed in terms of the path integral, which is an approach to statistical mechanics reminiscent of Feynman's path integral formulation of quantum mechanics. In this approach, one writes the partition function as a functional integral over fermionic paths:

$$Z = \operatorname{Tr} e^{-\beta H} = \int \mathcal{D}[c^\dagger, c]\; e^{-\int_0^\beta d\tau\; L},$$

from which many properties of the system may then be derived. Here, the equivalent *action* involves integration of the Lagrangian L over an imaginary time $\tau = it/\hbar$ with an upper limit of $\beta = \frac{1}{k_{\mathrm{B}}T}$.[2] Functional integration takes place over *coherent states* of the fields, such that all creation and annihilation operators within the integrand may be replaced by complex or *Grassman*[3] numbers for bosons or fermions, respectively.

Such a compact expression for the path integral hides a lot of complexity, however, since interacting Hamiltonians will generally involve non-quadratic terms that make this functional integral intractable. As it turns out, exact diagonalisation of the single-impurity Kondo model is actually possible, but relies on intensive *Bethe ansatz* techniques [4].

[1] $\vec{s}(0) = \frac{1}{2}\sum_{\boldsymbol{k},\boldsymbol{k}'}\sum_{\sigma,\sigma'} c^\dagger_{\boldsymbol{k},\sigma}\vec{\tau}_{\sigma,\sigma'}c_{\boldsymbol{k}',\sigma'}$, where $\vec{\tau}_{\sigma,\sigma'}$ is a vector of Pauli matrices.

[2] We shall set $k_{\mathrm{B}} = 1$ for the remainder of this project.

[3] These have the property of anti-commutation (among others), as described in [1].

2.4 Mean-Field Theory

The essence of mean-field theory is that we avoid performing the actual functional integration by approximating the integral by its saddle point, a step also known as the stationary phase approximation. In making this approximation, we are essentially imposing self-consistency conditions on whatever fields now appear in L, making them take on their mean values. Thankfully, these mean-field self-consistency equations are exactly what result from directly minimising the effective action. This step greatly reduces the complexity of the problem and so one can easily construct mean-field theories for magnetism or other well-known models such as BCS theory [1], for example. Mean-field theory also provides the minimal field configuration on top of which one could perturbatively include fluctuations to further understand the dynamics of a system.

To get to a mean-field theory description of the Kondo model, however, it is beneficial to first transform the non-quadratic Lagrangian into a more manageable form. The general strategy will be to add further auxiliary-fields to the path integral such that the partition function remains unchanged, with the foresight that this added complexity will not be too burdensome at mean-field level because it will only require more field minimisation. Such transformations often necessitate that hard constraints be applied in the form of Lagrange multipliers, which is what this new approach will seek to do differently.[4]

2.5 Read-Newns Approach to the Kondo Model

We now turn to mean-field theory in the context of the single-impurity Kondo model, starting with the established approach of Read and Newns [5].

2.5.1 Pseudo-Fermion Representation of Spin

Firstly, one requires a way to represent the localised spin degree of freedom within the path integral. A common way to do this is through an Abrikosov pseudo-fermion representation which, for a spin-$\frac{1}{2}$ magnetic impurity, is the mapping:

$$\hat{s}_z = \frac{1}{2}\left(f^\dagger_\uparrow f_\downarrow - f^\dagger_\downarrow f_\downarrow\right) \ , \quad \hat{s}_+ = f^\dagger_\uparrow f_\downarrow \ , \quad \hat{s}_- = f^\dagger_\downarrow f_\uparrow \ . \tag{2}$$

This representation is faithful provided a constraint is enforced that only one pseudo-fermion state may be occupied at a time,

$$f^\dagger_\uparrow f_\downarrow + f^\dagger_\downarrow f_\downarrow = 1, \tag{3}$$

[4]The way that constraints are usually implemented is shown in Appendix A.

picking out only the physical subspace of an otherwise enlarged Hilbert space.

Proceeding in this way leads to the antiferromagnetic interaction term becoming an interaction between conduction electrons and pseudo-fermions (with some shift in the chemical potential)

$$J\vec{S}\cdot\vec{s}(0) = -\frac{J}{2}\sum_{\sigma,\sigma'}\sum_{\boldsymbol{k},\boldsymbol{k'}} :\left(c^\dagger_{\boldsymbol{k},\sigma} f_\sigma\right)\left(f^\dagger_{\sigma'} c_{\boldsymbol{k'},\sigma'}\right): \ , \tag{4}$$

which is now compatible with the path integral formalism.

2.5.2 Hybridisation Field

Not being of bilinear form, the interaction of Eq (4) still leaves us unable to perform a simple Gaussian integral over the fermionic fields. As such, the next step of the Read-Newns approach is to use a Hubbard-Stratonovich [1] transformation to decouple this term, expressing the interaction in terms of a new bosonic field V instead. This has the effect of changing the interaction term in the Lagrangian to

$$J\vec{S}\cdot\vec{s}(0) \quad \rightarrow \quad \sum_{\boldsymbol{k},\sigma}\left[V^* c^\dagger_{\boldsymbol{k},\sigma} f_\sigma + V f^\dagger_\sigma c_{\boldsymbol{k},\sigma}\right] + 2\frac{V^* V}{J} \ , \tag{5}$$

where the path integral will now also involve an additional integral over this new hybridisation field V. (For our mean-field purposes we shall choose a gauge in which V is real.)

2.5.3 Order Parameter

This hybridisation leads on to the notion of an *order parameter* for the system, which will characterise the strongly- and weakly-coupled regimes. The form of Eq (5) is similar to a resonant-level model in which f_σ electrons hybridize with conduction electrons $c_{\boldsymbol{k},\sigma}$ in the Fermi sea. If we were to define a quantity $\Delta \propto |V|^2$, say, then this quantity would express the degree of hybridisation, since $\Delta \to 0$ would correspond to negligible tunnelling between the two states. In fact, within the resonant-level model, such a quantity $\Delta = \pi\rho|V|^2$ arises naturally as the width of resulting resonance in the density of states, if ρ is the density of states of conduction electrons otherwise.

We shall therefore use Δ as the order parameter, where a symmetry broken $\Delta \neq 0$ will indicate that the system is in a Kondo phase.

2.6 The Soft-Constraint Approach

We now briefly outline the principles behind this new approach to mean-field theory as originally proposed in [2].

Recall the hard constraint $\sum_\sigma f_\sigma^\dagger f_\sigma = 1$, required when transforming to a pseudo-fermion representation of the impurity spin, but consider reformulating this constraint as:

$$(1 - n_\uparrow - n_\downarrow)^2 = n_\uparrow n_\downarrow + (1 - n_\uparrow)(1 - n_\downarrow) = 0. \tag{6}$$

Implementing this into the Lagrangian is formally equivalent, but problematic within mean-field theory because one later imposes:

$$\langle (1 - n_\uparrow - n_\downarrow)^2 \rangle = 0 \, ,$$

which, for such a positive semi-definite operator, enforces the exact constraint and leads to a diverging mean-field parameter.[5]

A resolution to this issue is found by first introducing an auxiliary non-interacting (spin-less) fermion h that is constrained to be trivially empty through imposing $h^\dagger h = 0$ such as to have no physical effect. One then combines this constraint with that of Eq (6) by imposing instead:

$$n_\uparrow n_\downarrow + (1 - n_\uparrow)(1 - n_\downarrow) - K h^\dagger h = 0 \ , \tag{7}$$

where $K > 0, K \neq 1$ means that is no longer a positive semi-definite operator, leading to a realisable mean-field constraint. This encapsulates both constraints because the eigenvalues are now $\{1, \ 1 - K, \ 0, \ -K\}$ which still formally picks out the $h^\dagger h = 0$ and $(1 - n_\uparrow - n_\downarrow)^2 = 0$ subspaces within the path integral. Note that this has introduced an arbitrary parameter K into the problem and thus a new degree of freedom, but has allowed us to circumvent the issues related to the previous hard constraint within mean-field theory. For this reason, this approach to mean-field theory has been internally referred to as the *soft-constraint approach*.

2.7 Applying the Soft-Constraint to the Kondo Model

Though principles of the soft-constraint approach may find use in many problems in strongly correlated systems, this project is only concerned with its use in the context of the Kondo model, which will require the introduction of one more concept.

[5] Appendix B gives some feeling for why this is the case.

2.7.1 Kotliar-Ruckenstein Slave Bosons

One side effect of introducing the soft-constraint as we do in Eq (7) is that we have reintroduced non-quadratic terms such as $n_\uparrow n_\downarrow = f_\uparrow^\dagger f_\uparrow f_\downarrow^\dagger f_\downarrow$ which prevent us from integrating out the fermions. This can be resolved through the introduction of what are known as *slave bosons* [6] to represent each Fock state of the impurity fermions.

In particular, we shall use the representation of Kotliar and Ruckenstein (KR) [7] which utilises four bosons: e, $p_\uparrow$, $p_\downarrow$ and d to represent empty, singly- and doubly-occupied states, respectively. Again, for this representation to be faithful, one requires the following constraints to be satisfied:

$$e^\dagger e + \sum_\sigma p_\sigma^\dagger p_\sigma + d^\dagger d = 1 \quad \text{and} \quad f_\sigma^\dagger f_\sigma = p_\sigma^\dagger p_\sigma + d^\dagger d \, . \tag{8}$$

Additionally, the fermion operator must be suitably transformed so that bosonic occupations correctly correlate to the underlying fermionic states, achieved through:

$$f_\sigma \to \widetilde{z}_\sigma f_\sigma \, , \qquad \widetilde{z}_\sigma = e^\dagger p_\sigma + p_{-\sigma}^\dagger d \, . \tag{9}$$

This choice of $\widetilde{z}_\sigma$ within the path integral is not unique, yet does affect mean-field behaviour and so it is conventional to make the transformation

$$\widetilde{z}_\sigma \to z_\sigma = (1 - d^\dagger d - p_\sigma^\dagger p_\sigma)^{-1/2} \; \widetilde{z}_\sigma \; (1 - e^\dagger e - p_{-\sigma}^\dagger p_{-\sigma})^{-1/2} \, , \tag{10}$$

which recovers the exact behaviour in certain limits [6]. New dynamical terms for these bosons which will also appear in the Lagrangian shall become irrelevant when we look for the saddle point of the action.

2.7.2 The Soft-Constraint Lagrangian

Implementing the soft-constraint and KR bosons into the Read-Newns formulation, the final Lagrangian appearing in the path integral for this new approach becomes:

$$\begin{aligned} L_{\mathrm{SC}} \quad = \quad & \sum_{\boldsymbol{k},\sigma} c_{\boldsymbol{k},\sigma}^\dagger \left(\frac{d}{d\tau} + \epsilon_{\boldsymbol{k}} - \mu \right) c_{\boldsymbol{k},\sigma} + \sum_\sigma f_\sigma^\dagger \frac{d}{d\tau} f_\sigma + h^\dagger \frac{d}{d\tau} h \\ & + e^\dagger \frac{d}{d\tau} e + \sum_\sigma p_\sigma^\dagger \frac{d}{d\tau} p_\sigma + d^\dagger \frac{d}{d\tau} d \\ & + \sum_\sigma \lambda_\sigma (f_\sigma^\dagger f_\sigma - p_\sigma^\dagger p_\sigma - d^\dagger d) + \lambda_{\mathrm{KR}} (e^\dagger e + \sum_\sigma p_\sigma^\dagger p_\sigma + d^\dagger d - 1) \\ & + \lambda_{\mathrm{SC}} (e^\dagger e + d^\dagger d - K h^\dagger h) \\ & + 2 \frac{V V^*}{J} + \sum_{\boldsymbol{k},\sigma} \left(V^* c_{\boldsymbol{k},\sigma}^\dagger z_\sigma f_\sigma + V f_\sigma^\dagger z_\sigma^\dagger c_{\boldsymbol{k},\sigma} \right) \, . \end{aligned} \tag{11}$$

This contains every component needed to begin a mean-field theory analysis of the problem, since it is bilinear in fermionic fields.

2.7.3 Current Progress with the Soft-Constraint Approach

Thus far, investigation of the soft-constraint applied to the Kondo model has been restricted to zero temperature [2]. This has allowed for calculation of the zero temperature heat capacity and magnetic susceptibility and a corresponding ratio between the two known as the *Wilson ratio*.

One important feature of the soft-constraint approach is that it introduces an arbitrary free parameter into the problem, leaving the question of how it should be chosen. The freedom in K parametrises a whole family of mean-field solutions, and so it has been proposed that K could be tuned to match an established property of the system. One such property is the Kondo temperature T_K, which is known to be $T_K \approx D\sqrt{\rho J}e^{-1/(\rho J)}$ from a (two-loop) RG calculation, yet is overestimated by the Read-Newns approach which omits the $\sqrt{\rho J}$ factor.[6] This project shall therefore inherit this choice of K where applicable.

3 Finite-Temperature Study

As a first step towards constructing the temperature-field phase diagram, it is useful to gain some familiarity with the mean-field equations at finite temperature by investigating the Kondo model in the absence of a magnetic field. The isotropy of this zero-field case will allow for convenient simplification of some terms in the mean-field equations.

3.1 Obtaining the Mean-Field Equations

We start by deriving the self-consistency equations that must hold for the mean-field description of the system. Since $F = -T \ln Z$, searching for the minimal action is equivalent to directly minimising of F, illustrating a correspondence between the path integral and a more traditional way of approaching mean-field theory. Having introduced new bosonic fields to the Lagrangian of Eq (11), all fermionic fields may be integrated out as outlined in

[6] D is half the bandwidth of the conduction electrons, assumed to be large, and $\rho J \ll 1$.

Appendix C to obtain an effective free energy

$$\begin{aligned} F \quad = \quad & \overbrace{-2T\,\Re\sum_\sigma \ln\left[\frac{\widetilde{\Gamma}(\xi_\sigma+D)}{\widetilde{\Gamma}(\xi_\sigma)}\right]}^{F_0} + \frac{2\Delta}{\pi\rho J} - \sum_\sigma \lambda_\sigma(p_\sigma^2+d^2) \\ & + \lambda_{\mathrm{KR}}(e^2+\sum_\sigma p_\sigma^2+d^2-1) + \lambda_{\mathrm{SC}}(e^2+d^2) \underbrace{-T\ln\left(1+e^{\beta K\lambda_{\mathrm{SC}}}\right)}_{F_{\mathrm{h}}} \end{aligned} \tag{12}$$

in terms of the *gamma function* $\widetilde{\Gamma}(z) \equiv \Gamma(\frac{1}{2}+\frac{z}{2\pi iT})$ and $\xi_\sigma = \lambda_\sigma + iz_\sigma^2\Delta$, a complex resonance-level energy made slightly different by the inclusion of the KR term. The intermediate summation that gives rise to F_0 has been regulated by a cut-off D, the half-bandwidth, to reflect the fact that electrons of arbitrarily high energies do not exist within a metal.

Note that the temperature dependence of this free energy is solely contained in F_0 and F_{h}, which are the only terms that differ from the existing preliminary zero-temperature study of the soft-constraint approach. We now minimise this free energy to obtain a set of mean-field equations generalised to finite temperature, starting with the Hubbard-Stratonovich field

$$\frac{\partial F}{\partial \Delta} = 0 \implies \sum_\sigma \left[\frac{\partial F_0}{\partial \xi_\sigma} - \frac{\partial F_0}{\partial \overline{\xi_\sigma}}\right] iz_\sigma^2 = -\frac{2}{\pi J\rho}\ . \tag{13}$$

Though strictly free to only treat bosonic variables as complex numbers, we also restrict our search to real solutions, leading to one equation for each KR boson[7]:

$$\frac{\partial F}{\partial d} = 0 \implies \sum_\sigma \left[\frac{\partial F_0}{\partial \xi_\sigma} - \frac{\partial F_0}{\partial \overline{\xi_\sigma}}\right] \frac{\partial z_\sigma^2}{\partial d}\, i\Delta = -d\,(\lambda_{\mathrm{KR}}+\lambda_{\mathrm{SC}}-\sum_\sigma \lambda_\sigma)\ , \tag{14}$$

$$\frac{\partial F}{\partial e} = 0 \implies \sum_\sigma \left[\frac{\partial F_0}{\partial \xi_\sigma} - \frac{\partial F_0}{\partial \overline{\xi_\sigma}}\right] \frac{\partial z_\sigma^2}{\partial e}\, i\Delta = -e\,(\lambda_{\mathrm{KR}}+\lambda_{\mathrm{SC}})\ , \tag{15}$$

$$\frac{\partial F}{\partial p_\sigma} = 0 \implies \sum_s \left[\frac{\partial F_0}{\partial \xi_s} - \frac{\partial F_0}{\partial \overline{\xi_s}}\right] \frac{\partial z_s^2}{\partial p_\sigma}\, i\Delta = -p_\sigma\,(\lambda_{\mathrm{KR}}-\lambda_\sigma)\ . \tag{16}$$

The form of the ∂z_σ^2 derivative terms are irrelevant for the time being, but are found in Appendix D. Use of the chain rule means that the difficult derivative term

$$\frac{\partial F_0}{\partial \xi_\sigma} - \frac{\partial F_0}{\partial \overline{\xi_\sigma}} = \frac{i}{\pi}\Re(\widetilde{\psi}(\xi_\sigma+D) - \widetilde{\psi}(\xi_\sigma)) \tag{17}$$

appears repeatedly, where $\psi(z) \equiv \frac{d}{dz}(\ln\Gamma(z))$ defines the *digamma function*.

[7]This may be partly justified by the phase invariance of most terms apart from z_σ^2, which is also why we have dropped modulus-squared signs for the KR bosons throughout.

Finally, imposing Lagrange multiplier constraints completes the set of mean-field equations:

$$\frac{\partial F}{\partial \lambda_\sigma} = 0 \implies \left[\frac{\partial F_0}{\partial \xi_\sigma} + \frac{\partial F_0}{\partial \overline{\xi_\sigma}}\right] = (p_\sigma^2 + d^2) \ , \tag{18}$$

$$\frac{\partial F}{\partial \lambda_{\text{KR}}} = 0 \implies e^2 + \sum_\sigma p_\sigma^2 + d^2 = 1 \ , \tag{19}$$

$$\frac{\partial F}{\partial \lambda_{\text{SC}}} = 0 \implies e^2 + d^2 = K\langle h^\dagger h\rangle \equiv \kappa \ , \tag{20}$$

where the other combination of difficult derivatives is

$$\frac{\partial F_0}{\partial \xi_\sigma} + \frac{\partial F_0}{\partial \overline{\xi_\sigma}} = -\frac{1}{\pi}\Im(\widetilde{\psi}(\xi_\sigma + D) - \widetilde{\psi}(\xi_\sigma)) \ . \tag{21}$$

3.2 Solving the Mean-Field Equations

Our aim is to self-consistently satisfy the mean-field equations derived above. The absence of any magnetic field means that there is nothing to favour any particular configuration of the spin-$\frac{1}{2}$ magnetic impurity, so we should expect the existence of a solution with $p_\uparrow = p_\downarrow$ and $\lambda_\uparrow = \lambda_\downarrow$, allowing us to drop spin indices σ. Next, we shall make use of particle-hole symmetry to equate $e^2 = d^2$, which will dramatically simplify the mean-field equations.[8]

These simplifications mean that the occupation of each KR boson is entirely determined by κ as:

$$e^2 = d^2 = \frac{1}{2}\,\kappa \quad \text{and} \quad p^2 = \frac{1}{2}(1-\kappa) \ . \tag{22}$$

Subtracting Eq (15) and Eq (14) immediately implies $\lambda_\sigma = 0$, which means that the complex energy $\xi = iz^2\Delta$ is now purely imaginary. Combining Eq (18) and Eq (19) leads to

$$\frac{1}{2} = \frac{\partial F_0}{\partial \xi} + \frac{\partial F_0}{\partial \overline{\xi}} \approx -\frac{1}{\pi}\Im\left[\ln\frac{D}{2\pi i T} - \widetilde{\psi}(\xi)\right] \ ,$$

where we have used the large bandwidth $D \gg T, \xi$ to make the leading order approximation that $\psi(z) \approx \ln z$ for large z. Taking the principal value of the complex logarithm then leads to the result that

$$\Im\left[\psi\left(\frac{1}{2} + \frac{\xi}{2\pi i T}\right)\right] = 0 \ ,$$

which is merely consistent with the $\lambda_\sigma = 0$ conclusion that arose immediately from particle-hole symmetry and so tells us nothing new.

[8] Particle-hole symmetry comes out as a necessity in the Read-Newns mean-field approach, but here it is motivated by the belief that empty and doubly occupied pseudo-fermion states should be equally unphysical.

Turning to Eq (13) and making the same approximations, we may derive an implicit relation for Δ in terms of T and κ, similar to that found in [1]:

$$\psi\left(\frac{1}{2}+\frac{z^2\Delta}{2\pi T}\right)=\ln\frac{D}{2\pi T}-\frac{1}{J\rho z^2}\ . \tag{23}$$

Finding the finite temperature behaviour of the order parameter is therefore a case of inverting this relation for Δ, though it will not be possible to find an expression in terms of elementary functions.

3.2.1 Importance of $\lambda_{\mathrm{SC}} \geq 0$

In identifying $\kappa = K\langle h^\dagger h\rangle$ as a free parameter, we should be certain that $\lambda_{\mathrm{SC}} > 0$, since the thermal occupation of h takes on a familiar Fermi-Dirac form

$$\langle h^\dagger h\rangle = -\frac{1}{K}\frac{\partial F_{\mathrm{h}}}{\partial\lambda_{\mathrm{SC}}} = \frac{1}{1+e^{-\beta K\lambda_{\mathrm{SC}}}}\ .$$

If one were to find that $\lambda_{\mathrm{SC}} < 0$, then the zero-temperature limit would have $\langle h^\dagger h\rangle \to 0$, thereby nullifying any effect of the freedom to choose K.

Solving the remainder of the mean-field equations for λ_{SC}, we find that

$$\lambda_{\mathrm{SC}} = \frac{2\Delta}{\pi J\rho}\frac{1-2\kappa}{\kappa(1-\kappa)} \geq 0 \quad \text{for} \quad \kappa \leq \frac{1}{2} \tag{24}$$

which means $\langle h^\dagger h\rangle \in \left(\frac{1}{2},\ 1\right)$ and so we may indeed treat κ as our free parameter (for the time being).[9]

3.3 Zero-Temperature Heat Capacity

As a quick check of validity of the above solution, one hopes that the zero-temperature limit should reproduce the leading order temperature dependence obtained from expanding the Fermi function around $T = 0$, something that has already been done using the soft-constraint approach [2].

Knowing that this particular response function is derived from the free energy as $C = \frac{\partial E}{\partial T} = -T\frac{\partial^2 F}{\partial T^2}$, we start by finding the leading order behaviour of $\frac{\partial F}{\partial T}$ from the minimised form

[9] The added restriction on the magnitude of κ may be seen from Eq (22) to be equivalent to the seemingly reasonable statement that the physical pseudo-fermion states for the impurity should be more occupied than unphysical ones.

of the free energy:

$$F^\star = \underbrace{-4T\,\Re\,\ln\left[\frac{\widetilde{\Gamma}(iz^2\Delta + D)}{\widetilde{\Gamma}(iz^2\Delta)}\right]}_{F_0^\star} + \frac{2\Delta}{\pi J\rho} + \overbrace{\kappa\lambda_{\text{SC}} - T\ln\left(1 + e^{\beta K\lambda_{\text{SC}}}\right)}^{F_{\text{h}}^\star}\ . \tag{25}$$

It can be seen that the final term $F_{\text{h}}^\star \approx -\kappa\lambda_{\text{SC}}e^{-\beta K\lambda_{\text{SC}}}$ will vanish quickly as $T \to 0$ in comparison to the first two terms, so we may safely neglect this contribution at leading order in T.

Anticipating that explicitly calculating the inverse of Eq (23) will be somewhat difficult, we may find an expression for $\frac{d\Delta}{dT}$ by inverting the chain rule

$$\frac{d\psi}{dT} = \frac{d\psi}{du}\frac{\partial u}{\partial\Delta}\frac{d\Delta}{dT} + \frac{d\psi}{du}\frac{\partial u}{\partial T} \implies \frac{d\Delta}{dT} = \left(\frac{d\psi}{dT}\left[\frac{d\psi}{du}\right]^{-1} - \frac{\partial u}{\partial T}\right)\left[\frac{\partial u}{\partial\Delta}\right]^{-1}, \tag{26}$$

where $u \equiv \frac{1}{2} + \frac{z^2\Delta}{2\pi T}$ denotes the argument of $\psi(u)$. Thus, the only non-trivial derivative term left to calculate is $\left[\frac{d\psi}{du}\right]^{-1}$ which, using the asymptotic expansion of $\ln\Gamma(u)$ [10], is

$$\left[\frac{d\psi}{du}\right]^{-1} = u - \frac{1}{2} + \frac{1}{12u} + \dots\ .$$

This gives the leading-order temperature dependence of the order parameter as

$$\frac{d\Delta}{dT} \approx -\frac{\pi^2}{3}\frac{T}{z^4\Delta}\ , \tag{27}$$

reproducing a previous result in [2]. Upon combining all derivative terms (as outlined in Appendix E), the zero-temperature heat capacity is found to be

$$C = \frac{2\pi}{3}\frac{T}{z^2\Delta}\ , \tag{28}$$

once again reassuringly consistent with the result obtained from the first-order correction to the Fermi function [2]. The finite temperature mean-field equations therefore provide an alternative derivation of this limit of the heat capacity.

3.4 Plotting the Mean-Field Solution

Satisfied that the zero-temperature limit of Eq (23) reproduces familiar results, we may use this implicit equation to plot the temperature dependence of the Δ in the case of κ being constant[11], as shown in Figure 2.

[10] The asymptotic expansion of $\ln\Gamma(u)$, known as *Stirling's series*, is given by [8]

$$\ln\Gamma(u) = \frac{1}{2}\ln 2\pi + u(\ln u - 1) - \frac{1}{2}\ln u + \frac{1}{12u} - \frac{1}{360u^3} + \dots\ .$$

[11] Here, κ is once again chosen such that $z^{-2} = 1 - \frac{1}{2}\rho J\ln(\rho J)$ to reproduce $T_K = D\sqrt{\rho J}e^{-1/(\rho J)}$ [2].

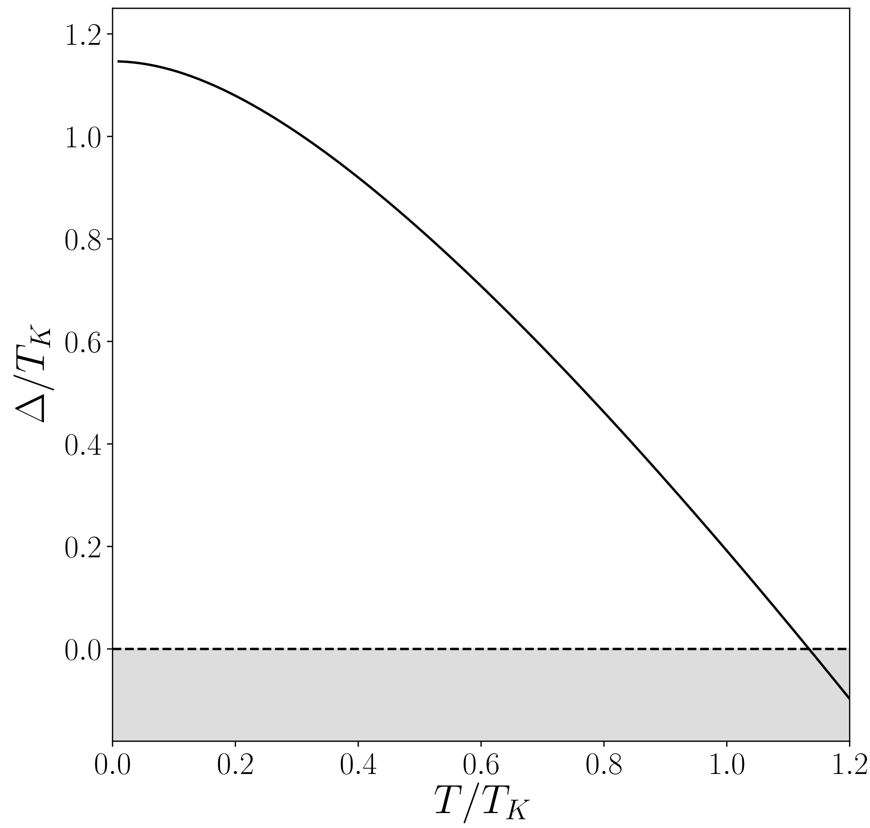

Figure 2: A plot of the order parameter Δ against the temperature T, with both axes normalised by the Kondo temperature T_K. The shaded region below the $\Delta = 0$ line indicates a non-physical region of the order parameter. The phase transition occurs at $T_c \approx 1.13\ T_K$.

From this plot it may be seen that the first derivative of the order parameter, $\frac{d\Delta}{dT}$, is discontinuous at $T = T_c$ if intervening by not allowing Δ to become negative. This has the consequence (see Appendix H) that $\frac{d^2F}{dT^2}$ is also discontinuous, characteristic of a second-order phase transition as opposed to a crossover. (Section 3.6 will investigate whether judiciously choosing the temperature dependence of the original soft-constraint parameter $K \to K(T)$ can remove this phase transition.)

3.5 Limitations of a Constant Soft-Constraint Parameter

Before starting to artificially influence the temperature dependence of the model by promoting $K \to K(T)$, one might question whether or not this is a natural thing to do in the first place. In solving the mean-field equations as we did in Section 3.2, we absorbed the analytically difficult $\langle h^\dagger h \rangle$ term into a free parameter κ that allowed us to reduce the mean-field equations to a single equation, namely Eq (23). This strategy, however, came at the cost of expressing Δ in terms of κ and *not* the elementary parameter K which originally appeared in the introduction to the soft-constraint approach. We shall now observe the behaviour that would arise if insisting that K were instead held *constant*.

Keeping the mean-field equations in terms of K and T, we are left to solve two simultaneous equations involving λ_{SC} and Δ:

$$\psi\left(\frac{1}{2} + \frac{z^2\Delta}{2\pi T}\right) = \ln\frac{T_K}{T} - \ln\left(2\pi\sqrt{\rho J}\right) + \frac{1}{\rho J}\left[1 - \frac{1}{z^2}\right] , \tag{29}$$

$$\lambda_{\mathrm{SC}} = \frac{8}{\pi\rho J}\frac{\Delta}{z^2}\left(1 - \frac{2K}{1 + e^{-\beta K \lambda_{\mathrm{SC}}}}\right) , \tag{30}$$

where $z^2 = 4K\left(1 - K/(1 + e^{-\beta K\lambda_{\mathrm{SC}}})\right) / \left(1 + e^{-\beta K\lambda_{\mathrm{SC}}}\right)$. It may be appreciated that simply rearranging these equations for Δ is now made impossible.

Nevertheless, it is still possible to make some progress by parameterising the above equations in terms of $s \equiv \beta\lambda_{\mathrm{SC}}$, and plotting the quantities Δ/T_K and T/T_K along both axes according to:

$$\left(\frac{T}{T_K}\right) = \frac{1}{2\pi\sqrt{\rho J}}\, e^{(1-z^{-2})/(\rho J)}\, \exp\left[-\psi\left(\frac{1}{2} + \frac{\rho J\ z^4\ s}{16(1 - 2K/(1 + e^{-Ks}))}\right)\right] , \tag{31}$$

$$\left(\frac{\Delta}{T_K}\right) = \frac{\pi\rho J\ z^2}{8(1 - 2K/(1 + e^{-Ks}))}\left(\frac{T}{T_K}\right) s . \tag{32}$$

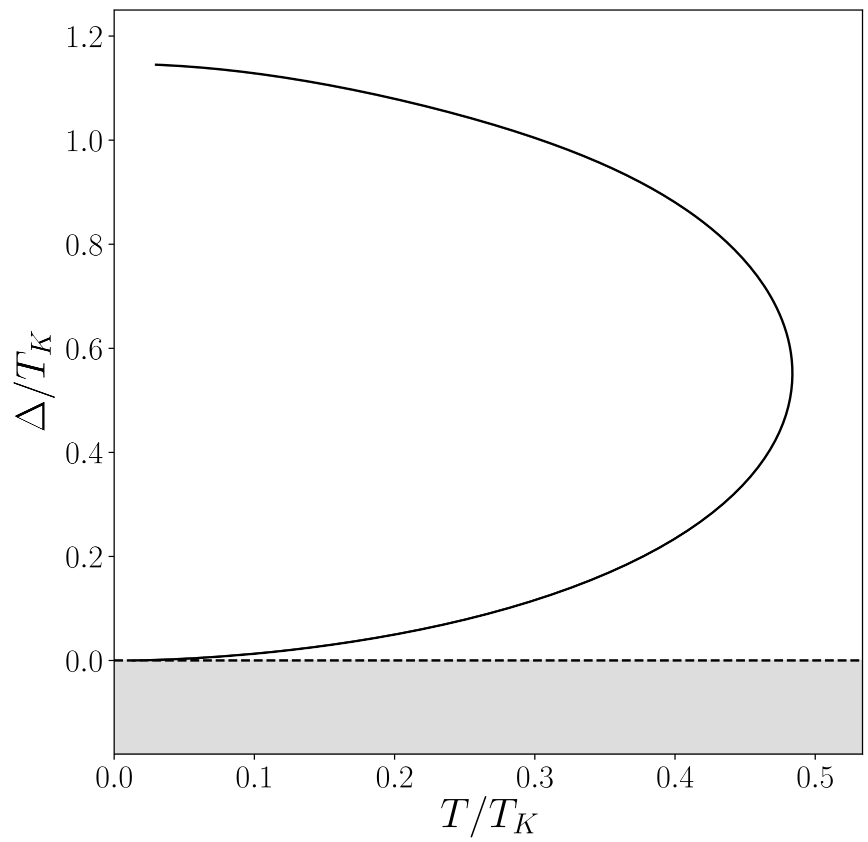

Figure 3: A plot of the order parameter Δ against the temperature T, produced parametrically for the case of constant K. The one-to-many mapping is not a physical function and so indicates a failure of the mean-field equations to pick out the minimal action.

The resulting parametric plot, Figure 3, has a catastrophic shape in which there are no mean-field solutions beyond a certain temperature, but two extremal values of Δ below this temperature.[12] This suggests a breakdown of the mean-field equations and from this clearly unphysical behaviour we conclude that K must indeed have some temperature dependence if it is to accurately describe any finite temperature features of the model at all.

3.6 Manipulating the Nature of the Phase Transition

We have seen that neither constant K nor κ can reproduce a crossover from a strongly-coupled to weakly-coupled phase at finite temperature. We now investigate whether a suitable choice of $\kappa \to \kappa(T)$ can remove this second-order phase-transition.

[12]This strange behaviour may look suspiciously like an artefact of the algebraic manipulations used to achieve the parametric form of Eq (31) and Eq (32) (such as s not being an injective parameterisation), but this functional form is also reproduced when numerically solving the mean-field equations.

The first question to ask is whether it is possible for mean-field Δ to only *asymptotically* approach the weakly-coupled phase as temperature is increased, thereby not assuming a piecewise form. Consider choosing a different value for the soft-constraint parameter $\widetilde{\kappa}$ such that $z^2 \to \widetilde{z^2} = \alpha z^2$. To see whether the form of $\Delta(T)$ will change significantly upon making this choice, one can look at the new mean-field equation for Δ:

$$\psi\left(\frac{1}{2} + \frac{\alpha z^2 \Delta}{2\pi T}\right) = \ln \frac{D}{2\pi T} - \frac{1}{J\rho\ \alpha z^2} \ . \tag{33}$$

When rescaling axes according to

$$\widetilde{T} = T \cdot e^{-\left(\frac{1}{\alpha}-1\right)/(J\rho z^2)} \ , \quad \widetilde{\Delta} = \Delta \cdot \alpha e^{-\left(\frac{1}{\alpha}-1\right)/(J\rho z^2)} \ , \tag{34}$$

this equation reduces to nothing more than the original mean-field equation of Eq (23), only this time in terms of $\widetilde{\Delta}$ and $\widetilde{T}$. Therefore, choosing a different constant value of κ cannot change the shape of $\Delta(T)$. Consequently, even if we promote $\kappa \to \kappa(T)$ [13], the above mean-field condition will have an unavoidable $\Delta = 0$ solution at some finite temperature below

$$T_c^\star = T_K \cdot e^{-\psi\left(\frac{1}{2}\right)} / \left(2\pi\sqrt{\rho J}\right) \ . \tag{35}$$

Another option is to attempt to match successive derivatives of Δ at the transition such that F will be continuous in all its derivatives. Trying to match all derivatives of a piecewise function that is analytic on both sides is conceptually dubious, however. This can be argued by saying that if all successive derivatives *were* chosen to match, then both sides would share a Taylor series expansion about that point and hence be described by the same function, without need for a piecewise definition. Unless resorting to non-analytic functions, increasing the order of the phase transition is the closest one could get to a crossover.[14]

With this in mind, we shall see what can nevertheless be achieved by choosing the form of $\kappa(T)$. For example, let κ_0 be the value of the soft-constraint parameter that correctly picks out the Kondo temperature as before.[15] Constructing $\kappa(T)$ as

$$\kappa(T) = \kappa_0 + \delta \cdot \left[\operatorname{sech}\left(\frac{T}{t_1}\right) + \tanh\left(\frac{T - T_c}{t_2}\right)\right] \ , \tag{36}$$

can allow the order parameter to more gradually approach $\Delta = 0$, as shown in Figure 4, provided that t_1, t_2 and δ are suitably chosen. The choice of the hyperbolic tangent above is somewhat arbitrary, but illustrates the principle that switching between $(\kappa_0 - \delta)$ and $(\kappa_0 + \delta)$ near the transition temperature can reduce the gradient to zero at the transition. (The

[13] After all, any temperature-dependent $\kappa(T)$ is just switching between different 'constant κ' curves.

[14] Empirically, all derivatives of Δ can be made to vanish by choosing $\frac{1}{J\rho z^2} = \frac{1}{J\rho z_0^2} - \ln\frac{T}{T_c}$, but this forces $\Delta = 0$ at all temperatures (clearly undesirable) and contradicts the existing limits on the magnitude of κ.

[15] $\kappa_0 = \frac{1}{2}\left(1 - \sqrt{-\frac{1}{2}\rho J \ln \rho J}\right)$

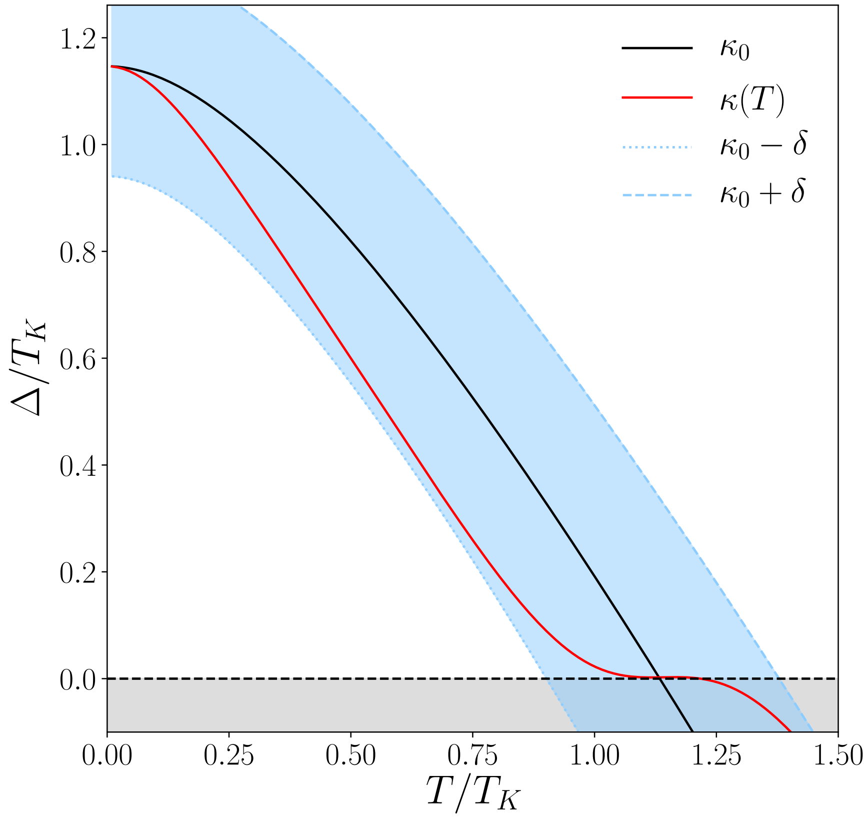

Figure 4: A plot where the form of $\kappa(T)$ is chosen to increase the order of the transition. Here, $\kappa(T)$ is given by Eq (38) (with $\delta \approx 0.018$, $t_1 \approx \frac{1}{5}T_K$ and $t_2 \approx \frac{4}{17}T_K$ for $\rho J = 0.16$) and switches from one constant κ curve to another. This allows the order parameter to take on any shape bounded by the blue shaded region, whose width is determined by the magnitude of δ.

hyperbolic secant term, on the other hand, serves to recover some of the zero-temperature behaviour.) There likely exist other, better choices for $\kappa(T)$, depending on the desired functional form of $\Delta(T)$; the only requirement is that $\frac{d\Delta}{dT} \to 0$ as $\Delta \to 0$, which can be achieved by tuning the parameters of the function such that

$$\frac{d\kappa}{dT}\Big|_{T=T_c} = \frac{4J\rho}{T_c}\frac{\kappa_0^2(1-\kappa_0)^2}{(1-2\kappa_0)} \quad \text{and} \quad \kappa(T_c) = \kappa_0 \ . \tag{37}$$

One glaring deficiency of this analysis is that it is still unclear how $K(T)$ should be chosen in the first place, since it would in general require solving

$$\kappa(T) = \frac{K(T)}{1 + e^{-\beta\lambda_{\mathrm{SC}}K(T)}} \ , \tag{38}$$

for which the simple relation $K(T) \approx 2\kappa(T)$ only holds near $T \approx T_c$. [16]

[16] For what it's worth, a solution can be approached through the infinite expression

$$K = \kappa\left(1 + \exp\left(-\beta\lambda_{\mathrm{SC}}\kappa\left(1 + \exp\left(-\beta\lambda_{\mathrm{SC}}\kappa\left(1 + \ldots\right)\right)\right)\right)\right) . \tag{39}$$

4 Finite Magnetic Field

Having explored the finite-temperature predictions for the soft-constraint in the absence of a magnetic field, we now introduce a finite magnetic field B which breaks the previous isotropy of the problem. One can include the effects of the magnetic field by introducing a Zeeman term for the magnetic impurity [9]:

$$F_B = -g\mu_B B \left(f_\uparrow^\dagger f_\uparrow - f_\downarrow^\dagger f_\downarrow \right) \cong -g\mu_B B \sum_\sigma \sigma p_\sigma^2 \ ,$$

where g is the *g-factor* and the effect on the conduction electrons is irrelevant at this scale.

4.1 Effect on the Mean-Field Equations

The inclusion of a magnetic field leaves the previous mean-field equations of Section 3.1 largely unchanged apart from the equation for the singly-occupied KR boson, which now becomes

$$\frac{\partial F}{\partial p_\sigma} = 0 \implies \sum_s \left[\frac{\partial F_0}{\partial \xi_s} - \frac{\partial F_0}{\partial \overline{\xi_s}} \right] \frac{\partial z_s^2}{\partial p_\sigma} \, i\Delta = -p_\sigma \left(\lambda_{\mathrm{KR}} - \lambda_\sigma - \sigma g\mu_B B \right) . \tag{40}$$

Without isotropy, however, solving the mean-field equations becomes appreciably more difficult, and so we will restrict ourselves to the slightly simpler task of searching for the location of the phase boundary $\Delta = 0$ in the $B - T$ plane because it allows particle-hole symmetry to be justifiably used again.

4.2 Plotting the Phase Boundary

Setting $\Delta = 0$, the mean-field Lagrange multipliers are found to be:

$$\lambda_{\mathrm{KR}} = 0 \ , \quad \lambda_{\mathrm{SC}} = 0 \ , \quad \lambda_\sigma = -\sigma g\mu_B B \ . \tag{41}$$

Proceeding with this fixed B-field, we obtain the condition that the occupancy of the impurity is given by

$$p_\sigma^2 = \frac{1}{2}(1-\kappa) + \sigma \frac{1}{\pi} \Im \left[\psi \left(\frac{1}{2} + \frac{g\mu_B B}{2\pi i T} \right) \right] , \tag{42}$$

which in the large B limit will have $\Im\left[\psi\left(\frac{1}{2} + \frac{g\mu_B B}{2\pi i T}\right)\right] \to -\frac{\pi}{2}$ such that $p_\downarrow^2$ becomes negative. Physically, this corresponds to one spin-state of the impurity being heavily favoured compared to the other, but this mean-field solution requires intervention with a piecewise definition to ensure that both p_σ^2 saturate sensibly.

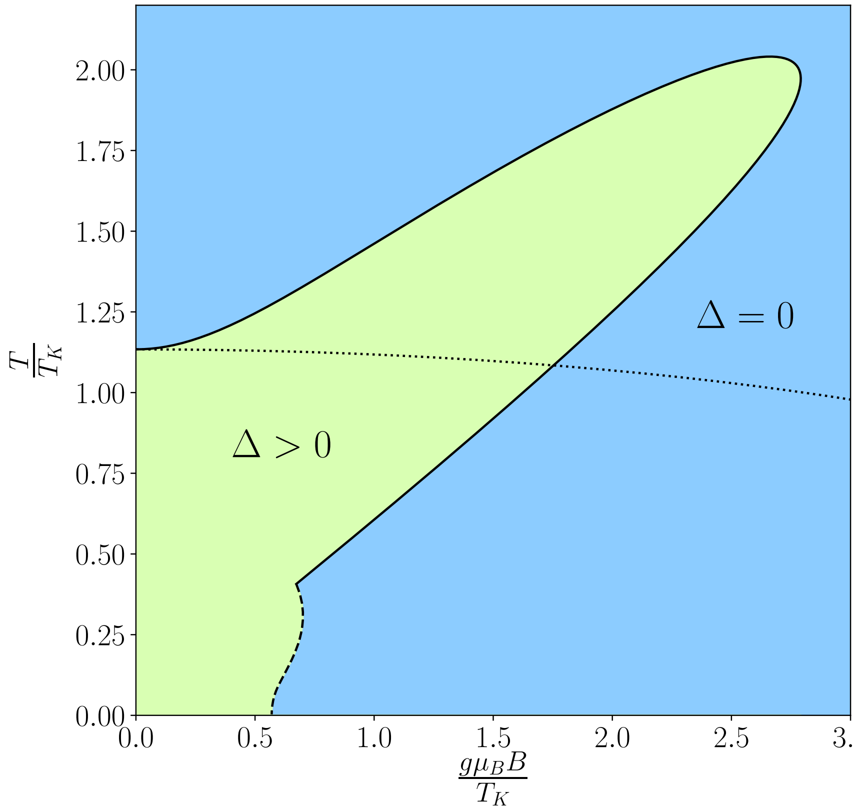

Figure 5: A phase diagram for the soft-constraint approach when κ held constant, generated parametrically using Eq (43). The shape of the boundary is highly sensitive to $z^2(\frac{B}{T})$, which is itself made to saturate by-hand beyond a certain value of $\frac{B}{T}$ and is plotted as a dashed line thereafter to indicate that it is no longer the true mean-field boundary. The dotted line shows the original large-N boundary of Figure 1.

Making a parametric plot of the phase boundary in terms of $b = \frac{g\mu_B B}{T}$ according to

$$\left(\frac{T}{T_K}\right) = \frac{1}{2\pi\sqrt{\rho J}} e^{\left(1-z^{-2}\right)/(\rho J)} \exp\left[-\Re\, \psi\left(\frac{1}{2} + \frac{b}{2\pi i}\right)\right] \quad \text{and} \quad \frac{g\mu_B B}{T_K} = \left(\frac{T}{T_K}\right) b \tag{43}$$

reveals a more worrisome problem with this approach, namely that the behaviour is dominated by the $\frac{1}{\rho J z^2}$ that appears in the exponential. If κ is left constant, then this leads to a phase boundary that curves upwards at large magnetic fields, as shown in Figure 5, because z^2 includes other field-dependent terms.[17] This is despite the fact that the rest of the expression behaves similarly to the large-N limit found by Piers Coleman [1], which was used to create the original phase diagram of Figure 1.

If one is truly interested in the case of the Kondo model subject to a fixed magnetic field, then it appears that κ would have to acquire a (likely complicated) B-field dependence

[17] This strange phase boundary does not arise if one is actually interested in the case where B is not fixed, but rather a uniformly distributed stochastic field $\widetilde{B} \in [-B/2,\ B/2]$, since the imaginary part of $\widetilde{\psi}(g\mu_B \widetilde{B})$ averages to zero and the same large-N limit of the phase boundary is recovered for constant κ.

to tame this unexpected behaviour. Given that it was only ever possible to increase the order of the phase transition in the absence of a magnetic field, it seems likely that a phase transition is also inevitable at finite fields. (Even the task of increasing the order of a phase transition is made much more challenging at finite field, and so has not been attempted in this project.)

5 Conclusion

This project aimed to explore the finite temperature and field behaviour of the Kondo model as predicted by a promising new variation of mean-field theory: the soft-constraint approach. Failure of conventional mean-field theories to accurately describe the phase diagram of this model makes it an ideal platform to test whether this new method is indeed a significant improvement that could find further use in describing strongly correlated systems.

The vast majority of effort was spent on the extension of this approach to finite-temperature, which was enough to draw some conclusions about the behaviour of the soft-constraint away from the $(T = 0,\ B = 0)$ point in the phase diagram. Crucially, it was found that the associated soft-constraint parameter has to be allowed to vary with temperature if it is to lead to a solvable set of mean-field equations. This is because the thermal occupancy of the auxiliary fermions introduced is enough to have a significant effect on the *effective* soft-constraint parameter in the mean-field equations.

Even when allowing the soft-constraint parameter to vary with temperature, a phase transition is found to be inevitable, in disagreement with the crossover obtained from other, more intensive methods. Nevertheless, it was demonstrated that artificially choosing the form of a temperature-dependent soft-constraint parameter can increase the order of the phase transition, though at the cost of zero-temperature accuracy.

The increased difficulty of the mean-field equations in the presence of a magnetic field meant that this aspect of the investigation was limited to a phase boundary calculation. These results suggest that the soft-constraint parameter would have to acquire further field dependencies to better describe the location and nature of the phase transition in the temperature-field plane.

A Constraints in the Lagrangian

The way that constraints can be implemented into the Lagrangian is illustrated in the following example. Suppose that we wanted to implement the constraint $\sum_\sigma f_\sigma^\dagger f_\sigma = 1$, say, which would be equivalent to having a partition function

$$Z = \mathrm{Tr}\left[e^{-\beta H} \ \delta\left(\sum_\sigma f_\sigma^\dagger f_\sigma - 1 \right) \right].$$

We could then express the constraint as

$$\delta\left(\sum_\sigma f_\sigma^\dagger f_\sigma - 1 \right) = \int_0^{2\pi} \frac{d\alpha}{2\pi} \ e^{-i\alpha(\sum_\sigma f_\sigma^\dagger f_\sigma - 1)} = \int_0^{2\pi i k_B T} \frac{d\lambda}{2\pi i k_B T} e^{-\beta\lambda(\sum_\sigma f_\sigma^\dagger f_\sigma - 1)},$$

where we have written $\lambda = i\alpha k_B T$. Absorbing various factors into the measure of integration, we may now write:

$$Z = \int \mathcal{D}[\lambda] \ \mathrm{Tr}\left[e^{-\beta H} e^{-\beta\lambda(\sum_\sigma f_\sigma^\dagger f_\sigma - 1)} \right].$$

Imposing this constraint can therefore be seen to be equivalent to modifying the original path integral and including an extra term in the Lagrangian:

$$L \to L + \lambda\left(\sum_\sigma f_\sigma^\dagger f_\sigma - 1 \right).$$

In fact, this is actually the Read-Newns constraint that is imposed on the occupation of the fermions f_σ (with $\sigma \in \{\uparrow, \downarrow\}$) representing the localised spin of the magnetic impurity.

B Divergent Mean-Field Parameter

To see why imposing $\langle (1 - n_\uparrow - n_\downarrow)^2 \rangle = 0$ leads to a divergent mean-field parameter, one may appreciate that by virtue of positive semi-definiteness, the mean-field condition

$$\left. \frac{\delta Z}{\delta \lambda(\tau)} \right|_{\bar{\lambda}} = 0$$

essentially becomes a condition on the integrand itself (namely something like $P e^{-\int d\tau \bar{\lambda} P} = 0$ for the constraint P), which forces $\bar{\lambda} \to \infty$.

C Deriving the Helmholtz Free Energy

The Lagrangian of Eq (11) now has all fermionic fields in quadratic form, by virtue of the new auxiliary bosons. One may therefore perform standard Gaussian integration over the

Grassman variables to get an expression involving the determinant of the action, following p.679 of [1]. Therefore, we get a block-diagonal form for the Lagrangian

$$L_{\mathrm{SC}} \quad = \quad \sum_{\sigma}\begin{pmatrix}\cdots & c^{\dagger}_{\boldsymbol{k},\sigma} & \cdots & f^{\dagger}_{\sigma}\end{pmatrix}\begin{pmatrix}(\epsilon_{\boldsymbol{k}}+\partial_\tau)\delta_{\boldsymbol{k},\boldsymbol{k'}} & V^* z_\sigma \\ \\ V z^{\dagger}_{\sigma} & (\lambda_\sigma+\partial_\tau)\end{pmatrix}\begin{pmatrix}\vdots \\ c^{\dagger}_{\boldsymbol{k'},\sigma} \\ \vdots \\ f^{\dagger}_{\sigma}\end{pmatrix} \quad + \quad \cdots$$

$$\implies F_{\mathrm{SC}} = -T\sum_{\sigma,n}\ln\det\begin{pmatrix}(\epsilon_{\boldsymbol{k}}-i\omega_n)\delta_{\boldsymbol{k},\boldsymbol{k'}} & V^* z_\sigma \\ \\ V z^{\dagger}_{\sigma} & (\lambda_\sigma - i\omega_n)\end{pmatrix} \quad + \quad \cdots \quad ,$$

which involves a summation over Matsubara frequencies ω_n. Note that this is almost identical to the standard Read-Newns expression but with $V \to V z^{\dagger}_{\sigma}$. The mean-field impurity electron contribution to the Helmholtz free energy is therefore

$$F = -T\sum_{\sigma,n}\ln\left(-i\omega_n + \lambda_\sigma + \sum_{\boldsymbol{k}}\frac{|z_\sigma|^2|V|^2}{i\omega_n - \epsilon_{\boldsymbol{k}}}\right) \quad + \quad \cdots \quad ,$$

where $\cdots$ now includes the conduction electron contribution and all the other constraint terms previously present in the Lagrangian. Contour methods give $\sum_{\boldsymbol{k}}\frac{|z_\sigma|^2|V|^2}{i\omega_n-\epsilon_{\boldsymbol{k}}} = -i|z_\sigma|^2\Delta\,\mathrm{sgn}\,\omega_n$, and so one may reuse the results of p.731 of [1] to rewrite this summation in terms of the gamma function after regulating the summation with the bandwidth D, leading to the free energy of Eq (12).

The auxiliary fermion contribution is already bilinear, and so may be integrated out using a standard Matsubara frequency summation:

$$L_{\mathrm{h}} = h^{\dagger}\left(\partial_\tau - K\lambda_{\mathrm{SC}}\right)h \implies F_{\mathrm{h}} = -T\sum_{n}\ln\left(-K\lambda_{\mathrm{SC}} - i\omega_n\right) = -T\ln\left(1+e^{\beta K\lambda_{\mathrm{SC}}}\right) .$$

D Further Details of the Mean-Field Equations

The derivatives of z^2_σ may be calculated quite easily as:

$$\frac{\partial z^2_\sigma}{\partial d} = \left(\frac{d}{1-d^2-p^2_\sigma} + \frac{p_{-\sigma}}{ep_\sigma + p_{-\sigma}d}\right)z^2_\sigma\ , \quad \frac{\partial z^2_\sigma}{\partial e} = \left(\frac{e}{1-e^2-p^2_{-\sigma}} + \frac{p_\sigma}{ep_\sigma + p_{-\sigma}d}\right)z^2_\sigma\ , \quad (44)$$

$$\frac{\partial z_\sigma^2}{\partial p_\sigma} = \left(\frac{p_\sigma}{1 - d^2 - p_\sigma^2} + \frac{e}{ep_\sigma + p_{-\sigma} d} \right) z_\sigma^2 \,, \quad \frac{\partial z_\sigma^2}{\partial p_{-\sigma}} = \left(\frac{p_\sigma}{1 - e^2 - p_\sigma^2} + \frac{d}{ep_\sigma + p_{-\sigma} d} \right) z_\sigma^2 \,. \quad (45)$$

The conjugate derivatives are also similar, but assuming the slave bosons to be purely radial as we do in this mean-field theory means that real expressions suffice.

E Deriving the Zero-Temperature Heat Capacity

The remaining derivative may be performed by using the same asymptotic expansion of the first line of

$$\begin{aligned} -\frac{1}{4}\frac{dF_0^\star}{dT} &= \Re \ln \widetilde{\Gamma}(iz^2\Delta + D) - \Re \ln \widetilde{\Gamma}(iz^2\Delta) - \Re\left[\frac{D}{2\pi i T}\, \widetilde{\psi}(iz^2\Delta + D) \right] \\ &+ \frac{z^2}{2\pi}\left(\frac{d\Delta}{dT} - \frac{\Delta}{T} \right) \Re\left[\widetilde{\psi}(iz^2\Delta + D) - \widetilde{\psi}(iz^2\Delta) \right] \,, \end{aligned}$$

where the second line has an exact expression from the mean-field equations Eq (13) and Eq (17). These come out to be:

$$\begin{aligned} \ln \widetilde{\Gamma}(iz^2\Delta + D) \quad &\approx \quad \frac{1}{2}\ln 2\pi - \frac{1}{2} + \left(\frac{z^2\Delta}{2\pi T} + \frac{D}{2\pi i T} \right)\left[\ln \frac{D}{2\pi i T} + \ln\left(1 + \frac{\pi i T}{D} + \frac{iz^2}{D} \right) - 1 \right] \\ &+ \frac{\pi i T}{6D}\left[1 + \frac{\pi i T}{D} + \frac{iz^2\Delta}{D} \right]^{-1} + \dots \,, \end{aligned}$$

$$\ln \widetilde{\Gamma}(iz^2\Delta) \approx \frac{1}{2}\ln 2\pi - \frac{1}{2} + \left(\frac{z^2\Delta}{2\pi T} \right)\left[\ln \frac{z^2\Delta}{2\pi T} + \ln\left(1 + \frac{\pi T}{z^2\Delta} \right) - 1 \right] + \frac{\pi T}{6z^2\Delta}\left[1 + \frac{\pi T}{z^2\Delta} \right]^{-1} + \dots \,,$$

$$\begin{aligned} \frac{D}{2\pi i T}\widetilde{\psi}(iz^2\Delta + D) \quad &\approx \quad \frac{D}{2\pi i T}\ln \frac{D}{2\pi i T} + \frac{D}{2\pi i T}\ln\left(1 + \frac{\pi i T}{D} + \frac{iz^2\Delta}{D} \right) \\ &- \frac{1}{2}\left(1 + \frac{\pi i T}{D} + \frac{iz^2\Delta}{D} \right)^{-1} - \frac{\pi i T}{6D}\left(1 + \frac{\pi i T}{D} + \frac{iz^2\Delta}{D} \right)^{-2} + \dots \,. \end{aligned}$$

Taking real parts and ignoring terms that are $\mathcal{O}(T^2)$ and $\mathcal{O}\left(\frac{1}{D^2}\right)$, this leads to

$$-\frac{1}{4}\frac{dF_0^\star}{dT} = -\frac{\pi}{6}\frac{T}{z^2\Delta} + \frac{1}{2\pi J\rho}\frac{d\Delta}{dT} + \dots \,, \tag{46}$$

which, incidentally, shows that we did not originally need to calculate the zero temperature limit of $\frac{d\Delta}{dT}$ because it cancels with this contribution.

F Impossibility of Asymptotically Approaching $\Delta = 0$

Even without making the large bandwidth approximation (which itself is a very good approximation for $\rho J \approx 0.2$), the mean-field condition

$$\Re\left[\psi\left(\frac{1}{2}+\frac{iz^2\Delta + D}{2\pi i T}\right)-\psi\left(\frac{1}{2}+\frac{iz^2\Delta}{2\pi i T}\right)\right]=\frac{1}{J\rho\, z^2}\ , \tag{47}$$

is incompatible with a limit in which $\Delta \to 0$ as $T \to \infty$, unless one could also have $z^2 = 4\kappa(1-\kappa)$ also diverging which, by the restriction on the magnitude of κ for validity of the soft-constraint approach, is forbidden. (Not that the Kondo model would be valid at such a temperature, in any case.)

G Obtaining $K(T)$ from $\kappa(T)$

We would like to know how to choose a $K(T)$, given that we have a functional form of $\kappa(T)$ in mind which also determines $\lambda_{\mathrm{SC}} = \lambda_{\mathrm{SC}}\left(\kappa(T),\ T\right)$.

By Eq (38), obtaining a closed form solution for $K(T)$ (through rearranging) is not in general possible, but a solution can be approached through the following infinite expression:

$$K = \kappa\left(1+\exp\left(-\beta\lambda_{\mathrm{SC}}\kappa\left(1+\exp\left(-\beta\lambda_{\mathrm{SC}}\kappa\left(1+\ldots\right)\right)\right)\right)\right). \tag{48}$$

H Relating $\frac{d^2F}{dT^2}$ to $\frac{d\Delta}{dT}$

The presence of the gamma function in the free energy means that an expression for the heat capacity $C = -T\frac{d^2F}{dT^2}$ will involve the derivative of the inverse digamma function and other such terms which are not expressible as elementary functions. (Not that these are numerically very challenging.) In this section, we seek to demonstrate that the assertion $\frac{d\Delta}{dT} = 0 \implies \frac{d^2F}{dT^2} = 0$ indeed holds as $\Delta \to 0$.

Taking a further derivative of $F_0^\star$, and allowing for the temperature dependence of $z^2(T)$, one obtains:

$$\begin{aligned}\frac{d^2F_0^\star}{dT^2}+\frac{2}{\pi J\rho}\frac{d^2\Delta}{dT^2} = &-\frac{2}{\pi\rho J z^2}\left[\Delta\frac{d^2z^2}{dT^2}+\frac{d\Delta}{dT}\frac{z^2}{dT}\right]+\frac{2z^2}{\pi T}\frac{d\Delta}{dT}+\frac{2\Delta}{\pi T}\frac{dz^2}{dT}\\ &+\frac{2\Delta}{\pi\rho J z^4}\left(\frac{dz^2}{dT}\right)^2-\frac{2\Delta}{\pi T\rho J z^2}\frac{dz^2}{dT}\ .\end{aligned}$$

From this expression it is clear that the right hand side will vanish if we make $\frac{d\Delta}{dT} = 0$ as $\Delta = 0$, thus this contribution to the free energy will be continuous in its second-derivative.

It now remains to check that this conclusion will also hold for the auxiliary system's contribution to the free energy $F^{\star}_{\mathrm{h}}$. This will require the observation that $\frac{d\Delta}{dT} = 0$ and $\Delta = 0$ together necessarily imply that $\frac{d\lambda_{\mathrm{SC}}}{dT} = 0$ and $\lambda_{\mathrm{SC}} = 0$, which follows from Eq (24). Taking the first derivative of gives:

$$\frac{dF^{\star}_{\mathrm{h}}}{dT} = \frac{d\kappa}{dT}\lambda_{\mathrm{SC}} - \ln\left(1 + e^{\beta K \lambda_{\mathrm{SC}}}\right) - \frac{T\lambda_{\mathrm{SC}}}{1 + e^{-\beta K \lambda_{\mathrm{SC}}}} \frac{d\left[\beta K\right]}{dT} . \tag{49}$$

Without explicitly taking a further derivative, it can be seen through the product rule that each term in $\frac{d^2 F^{\star}_{\mathrm{h}}}{dT^2}$ will have either λ_{SC} or $\frac{d\lambda_{\mathrm{SC}}}{dT}$ as a factor, both of which we have said vanish at the transition.

We have therefore shown that $\frac{d\Delta}{dT}\Big|_{T=T_c} = 0$ is a sufficient condition for $\frac{d^2F^{\star}}{dT^2}$ to be continuous at the transition. (This may seem like a trivial statement, but relied on some non-obvious cancellation of certain terms.)

I Code Excerpts

This section contains code used to plot figures in this report. Code for the entire project, along with version history, may be found in the following *GitHub* repository:

`https://github.com/ElisR/Kondo-Soft-Constraint`

I.1 Solving and Plotting the Equations in Parametric Form

```
# Trying to recreate previous plots without resorting to the Newton-Raphsen method

import numpy as np
import scipy.special as special
import scipy.optimize as optimize


global rho, J
rho = 0.4
J = 0.4


def MF_lambda_SC(Temp):
    """
    Solving for the Lagrange multiplier through brute force
    """

    K_T = 0.5 - 0.5 * np.sqrt(1 - 1 / (1 - 0.5 * rho * J * np.log(rho * J)))

    def MF_equation_lambda(lambda_SC, T):

```

```python
        k_T = K_T / (1 + np.exp(- K_T * lambda_SC / T))
        z2 = 4 * k_T * (1 - k_T)

        eq = special.digamma(0.5 + J * rho * z2 * z2 * lambda_SC /
                             (16 * T * (1 - 2 * k_T))) +\
            np.log(T) + np.log(2 * np.pi) +\
            0.5 * np.log(rho * J) - (1 - 1 / z2) / (rho * J)

        return eq

    return optimize.fsolve(MF_equation_lambda, 0, args=(Temp))


def F(s):
    """
    Returns the mean field free energy
    Function of the non-affine parameter
    """

    z2 = 4 * k(s) * (1 - k(s))
    D = np.exp(1 / (rho * J)) / np.sqrt(rho * J)

    F_orig = (s * z2 / (2 * (1 - 2 * k(s))) -
              4 * np.real(
        special.loggamma(0.5 +
                         s * J * rho * z2 * z2 / (16 * (1 - 2 * k(s))) +
                         D / (2 * np.pi * 1j * t(s))) -
        special.loggamma(0.5 +
                         s * J * rho * z2 * z2 / (16 * (1 - 2 * k(s)))))
              ) * t(s)

    F_extra = t(s) * (K(s) * s / (1 + np.exp(- K(s) * s)) -
                      np.log(1 + np.exp(- K(s) * s)))

    return (F_orig + F_extra)

def K(s):
    """
    Returns the value of the soft-constraint parameter
    """

    K_0 = 0.5 - 0.5 * np.sqrt(1 - 1 / (1 - 0.5 * rho * J * np.log(rho * J)))

    return K_0


def k(s):
    """
    Returns the value of the modified soft-constraint parameter
    Modification comes from thermal occupation of "empty" pseudo-fermions
    """

    return K(s) / (1 + np.exp(- K(s) * s))


def t(s):
    """
    Returns normalised temperature for given value of non-affine parameter
    """

    T = (1 / (2 * np.pi)) * (1 / np.sqrt(rho * J)) *\
        np.exp((1 - 1 / (4 * k(s) * (1 - k(s)))) / (rho * J)) *\
        np.exp(- special.digamma(
               0.5 + J * rho * s * np.square(k(s) * (1 - k(s))) /
               (1 - 2 * k(s))))

    return T


def delta(s):
    """
    Returns the mean-field hybridisation field at a given non-affine parameter
    """

    k_T = k(s)
    z2 = 4 * k_T * (1 - k_T)
```

```

    d = np.pi * J * rho * z2 * s * t(s) / (8 * (1 - 2 * k_T))

    return d
```

```
import New_Term_Parametric as parametric_SC

import numpy as np
import matplotlib.pyplot as plt


def plot_delta_vs_T():
    """
    Plotting delta vs T using a robust parametric plot, with extra term
    """

    ss = np.linspace(0, 250, 1500)

    ts = parametric_SC.t(ss)
    deltas = parametric_SC.delta(ss)

    fig = plt.figure(figsize=(8.4, 8.4))

    plt.rc('text', usetex=True)
    plt.rc('font', family='serif')

    plt.fill_between(np.linspace(-0.2, np.max(ts) + 0.2, 10),
                     0, -0.5, color='#dddddd')

    # Plot the figure
    plt.plot(ts, deltas, "k-")

    plt.xlabel(r'$ T / T_K $', fontsize=26)
    plt.ylabel(r'$ \Delta / T_K $', fontsize=26)

    ax = plt.gca()
    ax.set_xlim([0, np.max(ts) + 0.05])
    ax.set_ylim([-0.18, 1.25])
    ax.tick_params(axis='both', labelsize=20)

    plt.axhline(y=0, linestyle='--', color='k')


    plt.savefig("new_delta_vs_T_parametric.pdf",
                dpi=300, format='pdf', bbox_inches='tight')
    plt.clf()


def plot_F_vs_T():
    """
    Plotting the free energy against temperature
    """

    ss = np.linspace(0, 45, 1000)

    ts = parametric_SC.t(ss)
    Fs = parametric_SC.F(ss)

    fig = plt.figure(figsize=(8.4, 8.4))

    plt.rc('text', usetex=True)
    plt.rc('font', family='serif')

    plt.plot(ts, Fs, "k-")

    plt.xlabel(r'$ T / T_K $', fontsize=26)
    plt.ylabel(r'$ F / T_K $', fontsize=26)

    ax = plt.gca()
    ax.tick_params(axis='both', labelsize=20)

    plt.savefig("new_F_vs_T_parametric.pdf",
                dpt=300, format='pdf', bbox_inches='tight')
    plt.clf()
```

```python


def plot_lambda_vs_T():
    """
    Trying to ascertain form of lambda_SC against temperature
    """

    Ts = np.linspace(0.2, 1.2, 250)

    lambdas = np.zeros(np.size(Ts))

    ss_parametric = np.linspace(0, 45, 1000)
    ts = parametric_SC.t(ss_parametric)
    lambdas_parametric = np.multiply(ss_parametric, ts)

    for i in range(np.size(Ts)):
        T = Ts[i]

        lambdas[i] = parametric_SC.MF_lambda_SC(T)

    fig = plt.figure(figsize=(8.4, 8.4))

    plt.rc('text', usetex=True)
    plt.rc('font', family='serif')

    plt.plot(Ts, lambdas, "r-", label="fsolve")
    plt.plot(ts, lambdas_parametric, "k--", label="parametric")

    plt.xlabel(r'$ T / T_K $', fontsize=26)
    plt.ylabel(r'$ \lambda $', fontsize=26)

    ax = plt.gca()
    ax.tick_params(axis='both', labelsize=20)
    ax.legend()

    plt.savefig("s_vs_T.pdf",
                dpi=300, format='pdf', bbox_inches='tight')


def plot_eq_vs_lambda():
    """
    Investigating the nature of the MF equation
    """

    T = 0.6

    lambdas = np.linspace(-20, 20, 250)

    eqs = np.zeros(np.size(lambdas))

    for i in range(np.size(eqs)):
        eqs[i] = MF_equation_lambda(lambdas[i], T)

    fig = plt.figure(figsize=(8.4, 8.4))

    plt.rc('text', usetex=True)
    plt.rc('font', family='serif')

    plt.plot(lambdas, eqs, "r-", label=("T = " + str(T)))

    plt.xlabel(r'$ \lambda $', fontsize=26)
    plt.ylabel(r'$ MF_{eq}(\lambda) $', fontsize=26)

    ax = plt.gca()
    ax.tick_params(axis='both', labelsize=20)
    ax.legend()

    plt.savefig("eq_vs_lambda.pdf",
                dpi=300, format='pdf', bbox_inches='tight')


def main():
    # Setting various parameters of the problem

    global rho, J
    rho = 0.4
```

```python
    J = 0.4

    plot_delta_vs_T()
    plot_F_vs_T()


if __name__ == '__main__':
    main()
```

I.2 Plotting the Smoothed $\Delta(T)$

```python
# Exploring the effect of the new terms in the mean-field equations

import numpy as np
import matplotlib.pyplot as plt
import scipy.special as special
import scipy.optimize as optimize

import matplotlib.colors as colors
import matplotlib.cm as cmx


def digamma_inv(y):
    """
    Inverse digamma function
    Returns x given y: psi(x) = y
    """

    start = (np.exp(y) + 0.5) if (y >= -2.22) else (-1 / (y + special.digamma(1)))

    def inv(x):
        return special.digamma(x) - y

    return np.max(optimize.fsolve(inv, start))


def MF_delta(T, k_T):
    """
    Find the value of delta predicted by the mean-field equations
    """

    z2 = 4 * k_T * (1 - k_T)

    # This line previously had a huge error in it
    psi_tilde = - np.log(2 * np.pi) - np.log(T) - 0.5 * np.log(rho * J) + (1 - 1 / z2) / (rho * J)

    argument_tilde = digamma_inv(psi_tilde)
    delta = (argument_tilde - 0.5) * (2 * T * np.pi / z2)

    #return (delta >= 0) * delta
    return delta


def MF_lambda_SC(Temp):
    """
    Solving for the mean-field value of _SC at particular temperature
    i.e. Finds the root of MF_equation_lambda()
    """

    def MF_equation(lambda_SC, T):

        K_T = K(T)

        k_T = K_T / (1 + np.exp(- K_T * lambda_SC / T))

        constant_part = np.pi * J * rho * lambda_SC / 2
        difficult_part = MF_delta(T, k_T) * (1 - 2 * k_T) / (k_T * (1 - k_T))

        return constant_part - difficult_part

    MF_lambda_SC = optimize.fsolve(MF_equation, 0, args=(Temp))
```

```python

    return MF_lambda_SC


def F(T, delta, lambda_SC, k_T):
    """
    Return the value of the free energy for temperature, hybridisation field
    """

    f_original = 2 * delta / (np.pi * J * rho) - 4 * T * np.real(
        np.log(special.gamma(0.5 +
                             (1j * z2(T, k_T) * delta +
                              np.exp(1 / (rho * J)) / np.sqrt(rho * J)) /
                             (2j * np.pi * T)) /
               special.gamma(0.5 + (z2(T, k_T) * delta /
                                    (2 * np.pi * T)))))

    f_extra = lambda_SC * k_T - T * np.log(1 + np.exp(K(T) * lambda_SC / T))

    f = f_original + f_extra

    return f


def MF_F(T):
    """
    Return the mean-field free energy at a given temperature
    """

    # Set the soft-constraint parameter
    K_T = K(T)

    # Calculate the Lagrange multiplier
    lambda_SC = MF_lambda_SC(T, K_T)

    # Include the temperature dependent occupation
    k_T = k(lambda_SC, T, K_T)

    # Calculate the value of the hybridisation field
    delta = MF_delta(T, k_T)

    f = F(T, delta, lambda_SC, k_T)

    return f


def K(T):
    """
    Returns the value for the soft-constraint parameter K
    This is the standard value
    """

    K_0 = 0.5 - 0.5 * np.sqrt(1 - 1 / (1 - 0.5 * rho * J * np.log(rho * J)))

    return K_0


def k(lambda_SC, T, K_T):
    """
    Returns the value of the temperature dependent
    """

    return K_T / (1 + np.exp(- K_T * lambda_SC / T))

def k_smooth(T):
    """
    Returns a value of (constant) kappa that smoothes phase transition
    """

    change = 0.018
    gradient = 4.25

    return (change / np.cosh(5 * T)) + K(T) + change * np.tanh(gradient * (T - np.exp(-special.digamma(0.5)) / (2 * np.pi)))


def plot_lambda_vs_T():
```

```python
    """
    Plotting the value of lambda against temperature
    Mainly for debugging the parametric plot
    """

    Ts = np.linspace(0.2, 1.2, 250)

    lambdas = np.zeros(np.size(Ts))
    ss = np.zeros(np.size(Ts))

    for i in range(np.size(Ts)):
        T = Ts[i]

        lambdas[i] = MF_lambda_SC(T)
        ss[i] = lambdas[i] / T

    fig = plt.figure(figsize=(8.4, 8.4))

    plt.rc('text', usetex=True)
    plt.rc('font', family='serif')

    plt.plot(Ts, lambdas, "k-")
    plt.plot(Ts, ss, "r-")

    plt.xlabel(r'$ T / T_K $', fontsize=26)
    plt.ylabel(r'$ \beta \lambda $', fontsize=26)

    ax = plt.gca()
    ax.tick_params(axis='both', labelsize=20)

    plt.savefig("s_vs_T_solve_OG.pdf",
                dpi=300, format='pdf', bbox_inches='tight')


def plot_delta_vs_T():
    """
    Plots the *new* behaviour of the order parameter with temperature
    Includes the new temperature dependence of kappa
    """

    # Measure T in units of T_K
    Ts = np.linspace(0.01, 1.5, 250)

    lambdas = np.zeros(np.size(Ts))
    ks = np.zeros(np.size(Ts))

    deltas = np.zeros(np.size(Ts))
    deltas_up = np.zeros(np.size(Ts))
    deltas_down = np.zeros(np.size(Ts))

    deltas_interp = np.zeros(np.size(Ts))

    print("K = " + str(K(0.6)))
    for i in range(np.size(Ts)):

        T = Ts[i]

        deltas[i] = MF_delta(T, K(T))
        deltas_up[i] = MF_delta(T, K(T) + 0.018)
        deltas_down[i] = MF_delta(T, K(T) - 0.018)
        deltas_interp[i] = MF_delta(T, k_smooth(T))

    fig = plt.figure(figsize=(8.4, 8.4))

    plt.rc('text', usetex=True)
    plt.rc('font', family='serif')

    plt.fill_between(np.linspace(-0.2, np.max(Ts)+0.2, 10),
                     0, -0.5, color='#dddddd')

    plt.fill_between(Ts, deltas_up, deltas_down,
                     color='#8cccff', alpha=0.5)

    plt.plot(Ts, deltas, "k-", label=r'$ \kappa_0 $')
    plt.plot(Ts, deltas_interp, "r-", label=r'$ \kappa (T) $')
```

```
    plt.plot(Ts, deltas_down, ":", label=r'$ \kappa_0 - \delta $', color='#8cccff')
    plt.plot(Ts, deltas_up, "--", label=r'$ \kappa_0 + \delta $', color='#8cccff')


    plt.xlabel(r'$ T / T_K $', fontsize=26)
    plt.ylabel(r'$ \Delta / T_K $', fontsize=26)
    plt.legend(fontsize=22, frameon=False)

    ax = plt.gca()
    ax.set_xlim([0, np.max(Ts)])
    ax.set_ylim([-0.1, 1.1 * np.max(deltas)])
    ax.tick_params(axis='both', labelsize=20)

    plt.axhline(y=0, linestyle='--', color='k')

    plt.savefig("range_delta_vs_T.pdf", dpi=300,
                format='pdf', bbox_inches='tight', transparent=True)
    plt.clf()


def plot_graphical_solution():
    """
    Seeing how the implicit solution for lambda depends on delta
    """

    Ts = np.linspace(0.1, 1, 10)
    lambdas = np.linspace(0, 10, 100)

    linear_part = np.zeros((np.size(Ts), np.size(lambdas)))
    fermi_part = np.zeros((np.size(Ts), np.size(lambdas)))

    for i in range(np.size(Ts)):
        T = Ts[i]

        k_T = k(lambdas, T, K(T))
        delta = MF_delta(T, k_T)

        linear_part[i, :] = np.pi * J * rho * lambdas / (2 * delta)
        fermi_part[i, :] = (1 - 2 * k_T) / (k_T * (1 - k_T))

    # Plot the graphical solution, using colours
    cm = plt.get_cmap('inferno')
    cNorm = colors.Normalize(vmin=np.min(Ts), vmax=np.max(Ts))
    scalarMap = cmx.ScalarMappable(norm=cNorm, cmap=cm)

    fig = plt.figure(figsize=(8.4, 8.4))

    plt.rc('text', usetex=True)
    plt.rc('font', family='serif')

    for i in range(np.size(Ts)):
        colorVal = scalarMap.to_rgba(Ts[i])

        plt.plot(lambdas, linear_part[i, :],
                 label=r'$ \pi J \rho \lambda_{SC} / 2 \Delta $',
                 color=colorVal)
        plt.plot(lambdas, fermi_part[i, :],
                 label=r'$ (1 - 2 \kappa) / \kappa (1 - \kappa) $',
                 color=colorVal)

    plt.xlabel(r'$ \lambda_{SC} $', fontsize=26)
    plt.ylabel(r'$ f(\lambda_{SC}) $', fontsize=26)
    # plt.legend(loc='upper right', fontsize=26, frameon=False)

    ax = plt.gca()
    ax.tick_params(axis='both', labelsize=20)
    ax.set_ylim([0, 6])
    ax.set_xlim([0, 10])

    plt.savefig("lambda_graphical-solution.pdf", dpi=300,
                format='pdf', bbox_inches='tight')

    plt.clf()

```

```python

def plot_F_vs_T():
    """
    Plotting the free energy wrt temperature
    Can look at second derivative numerically
    """

    Tc = np.exp(- special.digamma(0.5)) / (2 * np.pi)
    Ts = np.linspace(0.05, Tc + 0.2, 1001)

    MF_Fs = np.zeros(np.size(Ts))

    for i in range(np.size(Ts)):
        T = Ts[i]
        MF_Fs[i] = MF_F(T)

    fig = plt.figure(figsize=(8.4, 8.4))

    plt.rc('text', usetex=True)
    plt.rc('font', family='serif')

    plt.plot(Ts, MF_Fs, "r-", label="Mean-Field C")

    plt.xlabel(r'$ T / T_K $', fontsize=26)
    plt.ylabel(r'$ F / T_K $', fontsize=26)

    ax = plt.gca()
    ax.set_xlim([0, np.max(Ts)])

    ax.tick_params(axis='both', labelsize=20)

    plt.savefig("new_F_vs_T.pdf", dpi=300, format='pdf', bbox_inches='tight')
    plt.clf()


def main():
    # Setting various parameters of the problem

    global rho, J
    rho = 0.4
    J = 0.4

    #plot_graphical_solution()
    plot_delta_vs_T()
    #plot_F_vs_T()
    #plot_lambda_vs_T()

if __name__ == '__main__':
    main()
```

I.3 Generating the New Phase Boundary

```python
# Trying to investigate the phase boundary with non-zero magnetic field

import numpy as np
import scipy.special as special


global rho, J
rho = 0.4
J = 0.4


def Tc_stochastic(b):
    """
    Defining the parametric T in terms of difficult expressions
    Calculated using a stochastic magnetic field
    """

    z_squared = z2_stochastic(b)

```

```python
    t = (1 / (2 * np.pi * np.sqrt(rho * J))) *\
        np.exp((1 - 1 / z_squared) / (rho * J)) *\
        np.exp(np.real(- 4j * np.pi * special.loggamma(0.5 + b / (4j * np.pi)) / b))

    return t

def Tc(b):
    """
    Defining the parametric T in terms of b and other quantities
    Not using a stochastic magnetic field
    """

    t = (1 / (2 * np.pi * np.sqrt(rho * J))) *\
        np.exp((1 - 1 / z2_saturated(b)) / (rho * J)) *\
        np.abs(np.exp(- special.digamma(0.5 + b / (2j * np.pi))))

    return t


def z2_stochastic(b):
    """
    Defining the KR operator for the case of a stochastic B field
    This essentially makes the function constant
    """

    K = 0.5 - 0.5 * np.sqrt(1 - 1 / (1 - 0.5 * rho * J * np.log(rho * J)))
    K = 2 * K

    return K * (2 - K) + 0 * b


def z2_sat(b):
    """
    Defining the KR operator in terms of a B-field parameter, but treating the high-B
    ↪ case more carefully
    """

    K = 0.5 - 0.5 * np.sqrt(1 - 1 / (1 - 0.5 * rho * J * np.log(rho * J)))
    K = 2 * K

    im_psi = np.imag(special.digamma(0.5 + b / (2j * np.pi)))
    diff_squared = np.square(0.5 - K / 4) - np.square(im_psi / np.pi)

    p2_up = (1 / 2 - K / 4) + im_psi / np.pi
    p2_down = (1 / 2 - K / 4) - im_psi / np.pi

    z_squared = 0
    if (p2_up <= 0 or p2_down <= 0):
        z_squared = (1 - K / 2) / (1 - K / 4)
    else:
        z_squared = (K / 4) * np.square(np.sqrt(p2_up) + np.sqrt(p2_down)) / ((K / 4 +
        ↪ p2_up) * (K / 4 + p2_down))

    return z_squared


z2_saturated = np.vectorize(z2_sat)
```

```python
import New_Phase_Boundary as boundary_SC

import numpy as np
import matplotlib.pyplot as plt

def plot_new_phase_boundary():

    # Prepare the array for parametric plot
    join = 1.654
    b1 = np.linspace(0.001, join, 2000)
    b2 = np.linspace(join, 180, 1000)
    b = np.concatenate((b1, b2))

    x = b * boundary_SC.Tc(b)
    y = boundary_SC.Tc(b)

    x_stochastic = b * boundary_SC.Tc_stochastic(b)
```

```python
    y_stochastic = boundary_SC.Tc_stochastic(b)

    z2s_stochastic = boundary_SC.z2_stochastic(b)
    z2s_saturated = boundary_SC.z2_saturated(b)

    #right = np.linspace(max(x), 5.8, 10)

    fig = plt.figure(figsize=(8.4, 8.4))

    plt.rc('text', usetex=True)
    plt.rc('font', family='serif')

    join_index = np.size(b1)
    # Plot the figure
    plt.plot(x[:join_index], y[:join_index], "k-", label="normal")
    plt.plot(x[join_index:], y[join_index:], "k--", label="normal")
    plt.plot(x_stochastic, y_stochastic, "k:", label="stochastic")

    plt.fill_between(np.linspace(0, 4, 10), 2.5, color='#8cccff')
    plt.fill_between(x, y, color='#d9ffb3')

    # Label the phases
    plt.text(0.4, 0.8, r'$ \Delta > 0 $', fontsize=26)
    plt.text(2.35, 1.2, r'$ \Delta = 0 $', fontsize=26)

    # Make improvements to the figure
    plt.ylabel(r'$ \frac{T}{T_K} $', fontsize=26)
    plt.xlabel(r'$ \frac{g \mu_B B}{T_K} $', fontsize=26)

    ax = plt.gca()
    ax.set_xlim([0, 3])
    ax.set_ylim([0, 2.2])
    ax.tick_params(axis='both', labelsize=20)

    plt.savefig("new_phase_diagram.pdf", dpi=300,
                format='pdf', bbox_inches='tight', transparent=True)
    plt.clf()

def main():

    plt_new_phase_boundary()


if __name__ == "__main__":
    main()
```

References

[1] P. Coleman *Introduction to Many Body Physics* Cambridge University Press (2015)

[2] G. Goldstein, C. Castelnovo and C. Chamon *Mean-Field Method for Handling Null Constraints on Positive-Semidefinite Operators* Draft (2017)

[3] J. Kondo *Resistance Minimum in Dilute Magnetic Alloys* Progress of Theoretical Physics, Volume 32, Issue 1, p.37–49 (1964)

[4] N. Andrei, K. Furuya, and J. H. Lowenstein *Solution of the Kondo Problem* Reviews of Modern Physics 55.2 (1983): 331-402

[5] N. Read, and D. M. Newns *A New Functional Integral Formalism for the Degenerate Anderson Model* Journal of Physics C: Solid State Physics 16.29 (1983)

[6] Frésard R., Kroha J. and Wölfle P. *The Pseudoparticle Approach to Strongly Correlated Electron Systems* Strongly Correlated Systems. Springer Series in Solid-State Sciences, vol 171. (2012)

[7] G. Kotliar and A. E. Ruckenstein *New Functional Integral Approach to Strongly Correlated Fermi Systems: The Gutzwiller Approximation as a Saddle Point* Phys. Rev. Lett. **57**, 1362 (1986)

[8] M. Abramowitz *Handbook of Mathematical Functions, With Formulas, Graphs, and Mathematical Tables* Dover Publications, Inc. (1974)

[9] P. Coleman *Large-N as a Classical Limit (*$1/N \approx \hbar$*) of Mixed Valence* J. Magn. Matter, vol. 47-48, p.323 (1985)